Experimental Section

Chemicals. Starting Materials. They were of commercial origin except for 2-bromoquinoline,[41] 2-iodoquinoline,[42] and 4-cyanobenzophenone.[31] 4-Cyanophenyl diethyl phosphonate was synthetized by the reaction of 4-chlorobenzonitrile with potassium diethyl phosphite in the presence of nickel chloride:[43] mp 31–33 °C; NMR ($CDCl_3$, Me_4Si reference) δ 1.33 (CH_3, t), 2.51 (CH_2, 2 q, $J_{CH_2-CH_3} = 7$ Hz, $J_{P-CH_2} = 9$ Hz), 7.7–8.2 (C_6H_4, m); mass spectrum, *m/e* 239 (33), 212 (27), 185 (100), 166 (93), 130 (43), 119 (37), 110 (33), 103–102 (60), 77 (15), 76 (22); IR ($CHCl_3$) 2220 (CN), 1120 (P=O), 1030 cm^{-1} ($P(OEt)_2$).

Nucleophiles. They were prepared in a manner similar to that in ref 7 for experiments in liquid ammonia. Tetraethylammonium cyanide (Fluka) was used in acetonitrile.

Solvents. Liquid ammonia was purified as previously described.[44,45] The supporting electrolyte was potassium bromide in 0.1 M concentration. Acetonitrile was distilled on calcium hydride before use. In acetonitrile the supporting electrolyte was tetrabutylammonium fluoborate (0.1 M).

Electrochemical Instrumentation. It was the same as those previously described in ref 7 for liquid ammonia and in ref 31 for acetonitrile.

Procedures. Induction of the reaction of 4-chlorobenzonitrile (1.55×10^{-2} M) with diethylphosphite (0.663 M) in liquid ammonia was performed in an electrolysis cell (50 mL); the working electrode was a platinum grid (15-cm^2 surface area) and the counterelectrode a platinum wire separated by a no. 4 glass frit. The temperature was −40 °C. The potential was set at −1.35 V for 2 min until 10^{-2} F were passed. The cell was then disconnected and the reaction was allowed to run for 10 min. The resulting product was extracted with ether after evaporation of liquid ammonia and identified by comparison (VPC, mass spectrometry) with an authentic sample prepared as described above. The yield was determined by gas chromatography (3% OV17, 1.5 m) and was found to be 100%.

Induction of the reaction of the cyanide ion (M) with 4-bromobenzophenone (10^{-2} M) was carried out in a three-necked flask containing 50 mL of deoxygenated acetonitrile kept under a nitrogen atmosphere. The flask was connected with an electrolysis cell containing 2×10^{-3} M of 4-cyanobenzophenone and 10^{-1} M tetrabutylammonium fluoborate in 10 mL of acetonitrile. This last solution was electrolyzed (−1.8 V vs. Ag/Ag^+ (0.01 M)) exhaustively and poured while being stirred into the flask with careful exclusion of oxygen. Samples were withdrawn through a septum at regular intervals (10 min), quenched by air, and titrated by liquid chromatography (RP18 column, elution with 50–50 acetonitrile–methanol, UV detection at 254 nm).

Acknowledgment. The work was supported in part by the CNRS (Equipe de Recherche Associée 309 "Electrochimie Moléculaire"). We thank Professor J. F. Bunnett (University of California in Santa Cruz) for very stimulating discussions on several questions raised in this paper.

---

(41) Butler, J. L.; Gordon, M. *J. Heterocycl. Chem.* **1975**, *12*, 1015.

(42) Barlin, G. B.; Benbow, J. A. *J. Chem. Soc., Perkin Trans. 2* **1975**, 298.

(43) Taus, P. *Chem. Ber.* **1970**, *103*, 2428.

(44) Herlem, M. *Bull. Soc. Chim. Fr.* **1967**, 1687.

(45) Herlem, M.; Minet, J. J.; Thiébault, A. *J. Electroanal. Chem.* **1971**, *30*, 203.

(46) Possible occurrence of another type of termination steps involving the disproportionation of $ArX^{-\cdot}$: $2ArX^{-\cdot} \rightarrow ArX + ArX^{2-}$ with the latter fragmenting to Ar^- and X^- as suggested by a reviewer is extremely unlikely as results from the electrochemistry of aryl halides. In most cases the cleavage of $ArX^{-\cdot}$ is fast enough not to allow the disproportionation to proceed. When not the case, the distance between the waves featuring the successive reduction of ArX into $ArX^{-\cdot}$ and ArX^{2-} is such[47] as to imply that the coproportionation is much largely favored thermodynamically as compared to disproportionation. The latter reaction as pulled by the further cleavage of ArX^{2-} is thus likely to be slow. Note in this respect that the other termination steps are either second-order reactions close to the diffusion limit or very fast pseudo-first-order reactions.

(47) Savéant, J. M.; Thiébault, A. *J. Electroanal. Chem.* **1978**, *49*, 335.

Low-Temperature Fluorination of Aerosol Suspensions of Hydrocarbons Utilizing Elemental Fluorine

James L. Adcock,* Kiyoshi Horita, and Ehrengard B. Renk

Contribution from the Department of Chemistry, University of Tennessee, Knoxville, Tennessee 37916. Received December 23, 1980

Abstract: This work describes a new concept in direct fluorination methodology and an apparatus designed to achieve conditions necessary for the rapid, continuous partial or complete fluorination of hydrocarbon molecules under controlled conditions of temperature and concentration. Results from the fluorination of neopentane are presented which indicate that although the degree of fluorination for a given set of conditions indicates a Gaussian distribution, investigation of specific isomers indicates significant deviations from statistical isomer distributions in fluorinated neopentanes. Photochemical assisted fluorinations of neopentane, 1,4-dioxane, cyclohexane, and 2,2-dimethyl-1,3-dioxolane are described which produce the perfluorinated analogues directly in good purity and in high yields.

The fluorination of hydrocarbon molecules by present technology is limited to a few distinct methodologies. In most cases the most appealing methods from the standpoint of reaction rate and scale-up operate in anhydrous hydrogen fluoride which reacts with many organic moieties (Swart's halogen-exchange reaction and Simon's electrochemical process),[1-5] utilize metal fluoride reagents which are expensive (AgF_2, HgF_2), give incomplete fluorination with increasing complexity of the structure of the molecule to be fluorinated (CoF_3, $KCoF_4$)[6,7] or operate at elevated temperatures, and produce generally lower yields of more complex molecules (Bigelow's "jet fluorination").[8-10] The "LaMar"

---

(1) R. D. Chambers, "Fluorine in Organic Chemistry", Wiley-Interscience, New York, 1973, p 22.

(2) J. H. Simons, U.S. Patent 2 500 000, 1950.

(3) J. Burdon and J. C. Tatlow, *Adv. Fluorine Chem.*, **1**, 77 (1967).

(4) J. H. Simons, *Trans. Electrochem. Soc.* **95**, 47 (1949).

(5) J. H. Simons in "Fluorine *Chemistry*", Vol. 1, Academic Press, New York, 1950, p 401.

(6) R. D. Fowler, W. B. Burford, J. M. Hamilton, R. G. Sweet, C. E. Weber, J. S. Kasper, and I. Litant in "Preparation, and Technology of Fluorine and Organo-Fluorine Compounds", C. Slesser and S. R. Schram, Eds., McGraw-Hill, New York, 1951, p 349.

(7) R. D. Bagnall, P. L. Coe, and J. C. Tatlow, *J. Fluorine Chem.*, **3**, 329 (1974).

(8) E. A. Tyczkowski and L. A. Bigelow, *J. Am. Chem. Soc.*, **77**, 3007 (1955).

0002-7863/81/1503-6937$01.25/0 © 1981 American Chemical Society

method developed by Lagow and Margrave[11-13] utilizes "long" reaction times and the high dilution of fluorine with helium which also acts as a heat sink. A later development in this process by Lagow, Maraschin, and Adcock[14-18] couples the high dilution and "long" reaction time with a low-temperature-gradient (LTG) reactor densely packed with "light" copper turnings. The "LTG" method produces good yields of highly branched fluorocarbons[14,15] and is generally useful for the fluorination of hydrocarbon ethers,[16] esters,[17] acid fluorides,[17],[18] acid anhydrides,[19] and cyclic amines.[20] It, however, works well only for molecules with appreciable solid-state volatility and crystallinity. Materials that form oils and glasses or have low solid-state volatility give considerably lower yields than the 30–80% yields obtained when more nearly ideal molecules are fluorinated. It is also a batch process which is generally suitable only for small scale syntheses.

All of the previously mentioned methodologies have serious limitations, and although some have been adopted for industrial scale production, clearly a simple, more nearly general fluorination method would be desirable. We would like to present what we believe is such a method.

Description of the Process

The significant successes of the LTG direct fluorination technique and the intrinsic simplicity of direct fluorination have led to a firm belief that a successful, general fluorination technique could be developed employing elemental fluorine. A critical analysis of the LTG reaction system produced a set of five conditions which we believe contribute to a high yield reaction. The conditions which we considered important are (a) fluorination of molecules in the crystalline state, (b) a very high reactant surface area exposed to gaseous fluorine, (c) low initial temperatures, (d) high initial dilution of fluorine gas, and (e) a highly efficient mechanism of heat dissipation.

The crystalline matrix reduces hydrocarbon radical recombinations when radicals are formed under "dilute" conditions. The crystalline matrix acts as an energy sink to dissipate reaction energies. A high reactant surface area promotes uniform attack by fluorine on all reactant molecules. Low temperatures reduce the vigor of reaction by an overall reduction in kinetic energy and by limiting the number of radical chain initiations. High initial dilution of fluorine reduces the overall reaction rate and reduces the likelihood of simultaneous attack by two fluorine molecules or radicals on adjacent sites on a molecule which would increase the degree of fragmentation. Effective heat dissipation would prevent the formation of "hot spots" and prevent combustion from occurring.[21]

These conditions, however, must be modified if one is to achieve high degrees of fluorination over a reasonable time span. The concentration of fluorine must be increased to maintain a good reaction rate as the reactant molecules become more highly fluorinated and a greater percentage of collisions are ineffective. It is also beneficial in this regard to increase the temperature. Since these conditions directly conflict with the desired initial conditions, their imposition must be separated in time or in space. The LTG system simply changes the applied temperature gradient and increases the fluorine concentration over time.

Separation of the perfluorination enhancing conditions from the initial conditions in space requires that the reactant be mobile. This mobile species may then be induced to pass through progressively warmer regions which have higher degrees of fluorine concentration. A gaseous reactant would be mobile, of course, but the desirability of limiting collisions between hydrocarbon radicals and thus limiting coupling reactions giving tars and oils dictates a condensed, preferably crystalline, phase. A liquid reagent stream does not allow for the uniform, rapid mixing of the very reactive gaseous elemental fluorine, thus preventing uniform, controlled attack and substitution of fluorine at every C–H bond.

In order to achieve gaslike mobility and retain crystallinity, it is necessary to produce extremely small solid particulates. These particulates may then be suspended and transported by using a carrier gas. These particulates possess extremely high surface area which permits uniform attack by gaseous elemental fluorine on the suspended reactant. Extremely effective heat dissipation may be achieved by using helium as the carrier. Multiple collisions of the reactant particulates with the helium carrier gas molecules dissipate heat rapidly. Excess energy is continuously carried by the helium atoms to the walls of the reactor.

Principles of aerosol production are well developed. Our initial design ideas were developed from study of existing technology for producing aerosols which were developed primarily as an adjunct of atmospheric and industrial hygiene studies. Descriptive passages by N. A. Fuchs and A. G. Sutugin,[22] R. D. Cadle,[23] and F. C. Goodrich[24] describe the requirements of generators capable of producing aerosols. A more recent paper by A. G. Sutugin describes a mixer-type generator which is generally applicable to the problem of steady-state aerosol production in a flow reactor.[25] The major difference between our own independently developed design and that described by Sutugin is the subambient temperature capability of our design and its incorporation into a flow-type reactor system.

The aerosol fluorination system designed to produce a controlled continuous stream of aerosol particulates includes the following components (Figure 1). A bed of sodium fluoride heated to 850 °C (A) sublimes highly dispersed NaF particles (average radius 17.5 Å[26]) into the helium carrier gas. These particles serve as condensation nuclei for the hydrocarbon condensation. The carrier gas is chilled to near −196 °C by passing through a liquid-nitrogen-cooled heat exchanger (B). The chilled carrier gas, helium in this embodiment, is mixed with a second gas stream containing the hydrocarbon vapor in a precise arrangement within the body of the generator (C). The hydrocarbon vapor in the stream produced by an evaporator device (D) will condense into aggregates around the sodium fluoride particles within the chilled carrier. The chilled aerosol is directly channeled into the reactor (E) where it is mixed with elemental fluorine in such a way as to produce uniform contact between the aerosol particles and elemental fluorine. The temperature of the reactor (E) is controlled by means of an integral heat exchanger which can provide variable temperatures from the cryogenic to the ambient range.

The aerosol generator system is of the evaporation–condensation type. It, however, seems likely that aerosol particulates generated by any mechanism, physical, chemical, or mechanical, would work equally well. It is the high surface area created by extensive subdivision of aggregates that is essential to the process.

---

(9) A. F. Maxwell, F. E. Detoro, and L. A. Bigelow, *J. Am. Chem. Soc.*, **82**, 5827 (1960).

(10) B. C. Bishop, J. B. Hynes, and L. A. Bigelow, *J. Am. Chem. Soc.*, **86**, 1827 (1964).

(11) J. L. Margrave and R. J. Lagow, *Chem. Eng. News*, 40 (1970).

(12) R. J. Lagow and J. L. Margrave, *Proc. Natl. Acad. Sci.*, **67**, 4, 8A (1970).

(13) R. J. Lagow and J. L. Margrave, *J. Polym. Sci.*, **12**, 177 (1974).

(14) N. J. Maraschin and R. J. Lagow, *J. Am. Chem. Soc.*, **94**, 8601 (1972).

(15) N. J. Maraschin and R. J. Lagow, *Inorg. Chem.*, **12**, 1459 (1973).

(16) J. L. Adcock and R. J. Lagow, *J. Org. Chem.*, **38**, 3617 (1973).

(17) J. L. Adcock and R. J. Lagow, *J. Am. Chem. Soc.*, **96**, 7588 (1974).

(18) J. L. Adcock, R. A. Beh, and R. J. Lagow, *J. Org. Chem.*, **40**, 3271 (1975).

(19) J. L. Adcock and R. J. Lagow, unpublished results.

(20) J. L. Adcock, B. D. Catsikis, J. W. Thompson, and R. J. Lagow, *J. Fluorine Chem.*, **7**, 197 (1976).

(21) R. J. Lagow and J. L. Margrave, *Prog. Inorg. Chem.*, **26**, 161 (1979).

(22) C. N. Davis, Ed., "Aerosol Science"; Academic Press, London and New York, 1966, Chapter 1.

(23) R. D. Cadle, "Particle Size, Theory and Industrial Applications", Reinhold, New York 1965.

(24) G. M. Hidy, "Aerosols and Atmospheric Chemistry", Reinhold Papers Contributed Kendall Award Symposium, American Chemical Society, Los Angeles, CA, March 28–April 2, 1971, Academic Press, New York and London, S. Shahriari, A. N. Sarmiento, and F. C. Goodrich, 1972. "The Kinetics of Growth of an Aerosol in a Flow Reactor", p 67.

(25) A. G. Sutugin, "Advances in Aerosol Physics", Vol. 4, V. A. Fedoseer, Ed., Israel Program for Scientific Translations, Jerusalem, 1971, translated from Russian in 1973, p 36.

(26) W. Espenscheid, E. Matijevic, and M. Kerker, *J. Phys. Chem.* **68**, 2831 (1964).

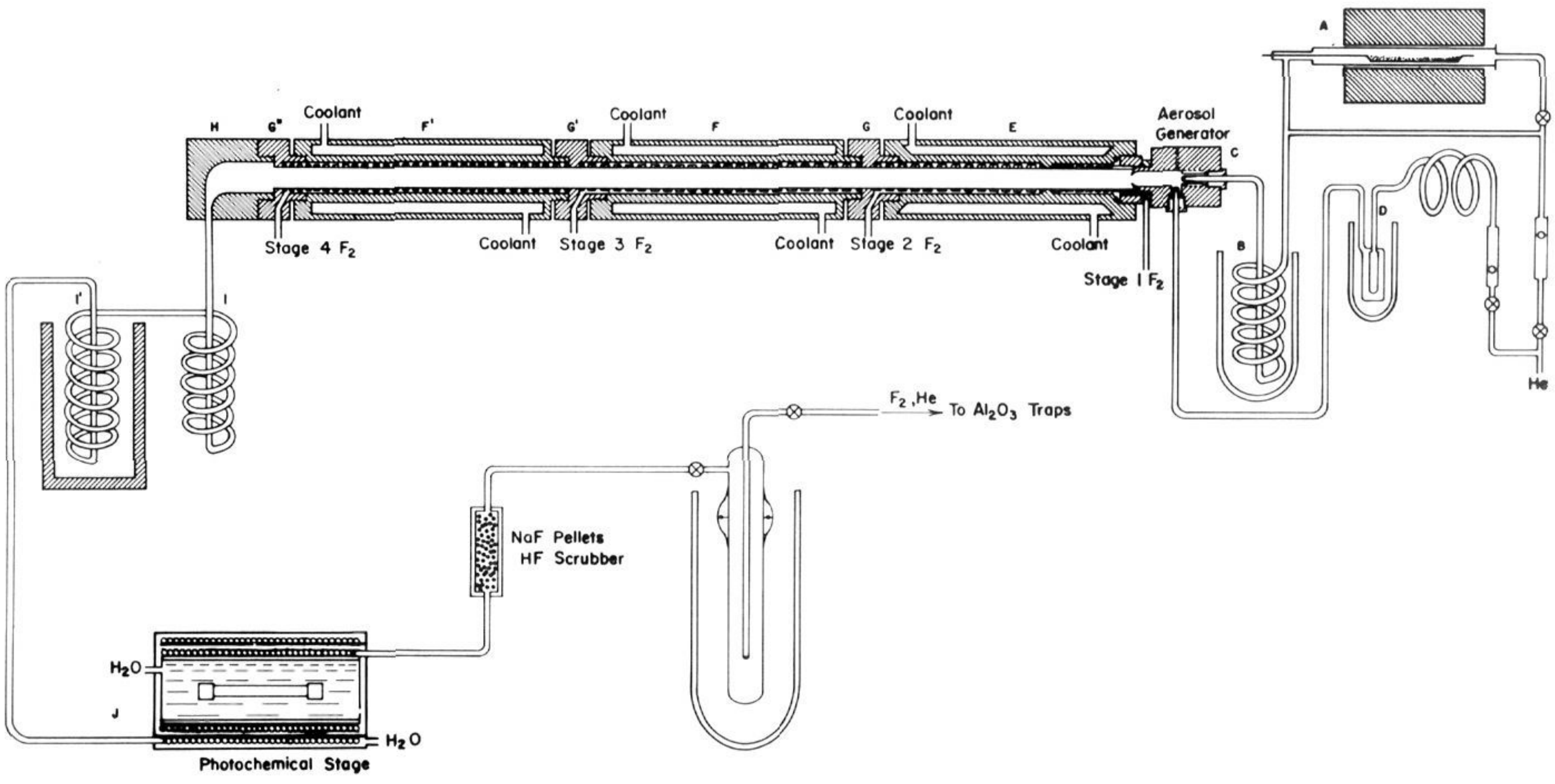

Figure 1. Aerosol fluorinator.

Having created a mobile reactant, it is possible to separate in space the conditions giving low fragmentation, i.e., high initial dilution of fluorine and low temperature, from those conditions leading to high degrees of fluorination, i.e., increased fluorine concentration and temperature.

Modular design of the system has allowed for the addition of staging components following the reactor (E). Each staging component consists of a module (F) and a "staging insert" (G). A series of modules (F′) connected to the reactor thus provide for independently controlled-temperature zones, and the addition of "staging inserts" (G′) allows the independently controlled injection of additional elemental fluorine. With use of these devices, hydrocarbon or other molecules may be controllably fluorinated to any degree including perfluorination. It is also conceivable that other reagents besides elemental fluorine can be introduced in the later stages to achieve functionalization etc.[27-29]

The addition of modules and staging inserts may be continued indefinitely by insertion ahead of the end cap (H). Each stage may be modified to provide for recycling of any or all of the various reacting species although this is not practical at the lab scale. In the system shown (Figure 1), a total of three staging inserts have been assembled, giving in effect a four-stage aerosol fluorination reactor in which fluorine can be added in four independently controlled zones at three independently controlled temperatures.[30]

In molecules which are exceptionally difficult to perfluorinate, a heated coil (I′) and/or a water-cooled flow-type photochemical reaction stage (J) following stage 4 (Figure 1) has been utilized to significantly activate the elemental fluorine and increase the reactant contact time before quenching. The photochemical stage allows exceptionally high yields of perfluorinated products as well as much more efficient utilization of elemental fluorine. Recent results exhibit perfluorination of neopentane using a 20% excess of fluorine.

The multistaged aerosol fluorination reactor achieves near optimum control over the potentially violent direct fluorination reaction. It is possible to expose the unfluorinated reactant to a very dilute, even distribution of elemental fluorine at low temperatures. Furthermore the condensed phase of the aerosol particle distributes reaction heat evenly over a large number of molecules held in an ideally crystalline aggregate which may readily dissipate energy by multiple rapid collisions with helium gas. All of these effects serve to reduce the violence and heat accumulation which are primary concerns in direct fluorination. As the reactant molecule becomes more highly fluorinated and hence less vulnerable, the aerosol aggregate is carried into regions of higher fluorine concentration, higher temperature, and generally more rigorous conditions which tend to bring about higher degrees of fluorination. Finally the highly fluorinated product mixture may be introduced into the photochemical stage to achieve maximum fluorination.

This combination of conditions, which allows independent control of reactant concentration, stoichiometry, temperature, and reaction time, is unique to the aerosol fluorination reactor. It is in effect a dynamic, variable-fluorine-concentration-gradient, variable-temperature-gradient reactor.

Description of the Experiments

Neopentane was purchased from K and K Laboratories, Inc., and was used as received. 1,4-Dioxane and cyclohexane (Fisher) were dried over Linde 4-A molecular sieve before use. 2,2-Dimethyl-1,3-dioxolane was prepared by allowing a 1:2 molar mixture of acetone–ethylene glycol to reflux over L-4A molecular sieve in the presence of paratoluene sulfonic acid for several days. The filtered liquid was run slowly into saturated aqueous potassium carbonate. The separated organic (top) layer was dried over L-4A sieves and fractionally distilled by using a spinning band distillation apparatus. The pure product (bp 89.0–90.0 °C, lit.[31] 90.0 °C) was collected in 11% yield although much more was collected as an apparent acetone azeotrope.

Elemental fluorine was purchased from Air Products Co. (97% technical grade, low oxygen content) in a cylinder containing 4.9 lb of F_2 at 400 psig. IR spectra were run on a Perkin-Elmer 257 grating spectrophotometer; mass spectra (electron-impact and chemical ionization) were obtained on a Hewlett-Packard 5980A mass spectrometer. ^{1}H and ^{19}F NMR were obtained from the South Carolina Magnetic Resonance Facility, Columbia, SC, operating under Grant NSF-CHE78-18723. Elemental analyses were performed by Schwarzkopf Microanalytical Laboratory, Woodside, NY. Mass throughput values for neopentane 1,4-dioxane, 2,2-dimethyl-1,3-dioxolane, and cyclohexane were calculated from empirical data.[30c] Gas chromatographic separations were made on a Bendix Model 2300 gas chromatograph with multilinear programing

---

[27] J. L. Adcock, Shoji Inoue, and R. J. Lagow, *J. Am. Chem. Soc.*, **100**, 1948 (1978); (b) U.S. Patent 4 114 374.

[28] J. L. Adcock, "Fluorine Sensitized Oxidation of Hydrocarbons", Presented at the 28th Southeast Regional Meeting of the American Chemical Society, Abstracts 451, 1976 and at the 174th National Meeting of the American Chemical Society, Chicago, IL, Aug 31, 1977, Abstract FLUO-22.

[29] J. L. Adcock, *J. Fluorine Chemistry*, **16**, 297 (1980).

[30] J. L. Adcock and E. B. Renk, "Low Temperature Fluorination of Aerosol and Condensed Phase Sol Suspensions of Hydrocarbons Utilizing Elemental Fluorine", Office of Naval Research: (a) Contract Technical Report No. 1, (b) No. 2, (c) No. 3.

[31] J. Gelas and S. Michaud, *Bull. Soc. Chim. Fr.*, 2445 (1972).

Table I. ^{19}F NMR Data of Fluorinated Neopentanes

			CF_3	CF_2H		CFH_2		
formula	ref no.	structure	ϕ,[a] ppm	ϕ,[a] ppm	*J*, Hz	ϕ,[a] ppm	*J*, Hz	integratn ratios
C_5H_{12}	*	$C(CH_3)_4$						
$C_5H_{11}F$	ND	$(CH_3)_3C\text{–}CFH_2$				222.7 (t)	46	
$C_5H_{10}F_2$	NL	$(CH_3)_2C(CFH_2)_2$				227.8 (t)	50.9	
$C_5H_{10}F_2$	NF'	$(CH_3)_3C\text{–}CF_2H$		~128[b] (d)	57.1			
$C_5H_9F_3$	NQ	$(CFH_2)_3C\text{–}CH_3$				234.6 (t)	49.6	
$C_5H_9F_3$	NK'	$(CH_3)_2C(CFH_2)(CF_2H)$		~131[b] (d)	53.4	~228[b] (t)	45.8	d:t ≈ 2:1
$C_5H_8F_4$	NS	$C(CFH_2)_4$				240.1 (t)	45.8	
$C_5H_8F_4$	NN	$(CH_3)_2C(CF_2H)_2$		129.2 (d)	53.4			
$C_5H_8F_4$	NO	$(CFH_2)_2C(CF_2H)(CH_3)$		132.7 (d)	53.4	236.3 (t)	45.8	d:t ≈ 1:1
$C_5H_2F_5$	NT	$(CFH_2)_3C\text{–}CF_2H$		131.1 (d)	53.4	241.1 (t)	45.8	d:t ≈ 2:3
$C_5H_6F_?$	NR	$(CFH_2)_2C(CF_2H)_2$		130.1 (d)	48.8	242.4 (t)	48.8	d:t ≈ 2:1
$C_5H_5F_7$	NP	$(CF_2H)_3C\text{–}CFH_2$		129.1 (d)	53.4	243.8 (t)	45.8	d:t = 6.8:1
$C_5H_4F_8$	NK	$C(CF_2H)_4$		128.4 (d)	53.4			
$C_5H_4F_8$	NI	$(CF_2H)_2C(CF_3)(CFH_2)$	66.8 (s)	129.3 (d)	51	244.4 (t)	41	s:d:t = 3:4:1
$C_5H_3F_9$	NH	$(CF_2H)_3C\text{–}CF_3$	64.5 (s)	127.8 (d)	51			s:d = 1:2
$C_5H_3F_9$	NG	$(CF_3)_2C(CFH_2)(CF_2H)$	66.57[c] (q)	130.1[c] (d)	52.2	240.4[c] (t)	45.6	
$C_5H_2F_{10}$	NE	$(CF_2H)_2C(CF_3)_2$	64.6[c] (p)	127.29 (d)	54.5			
C_5HF_{11}	NC	$(CF_3)_3C\text{–}CF_2H$	65.4[c] (t)	125.7	53			
C_5F_{12}	NB	$C(CF_3)_4$	65.42[c] (s)					

[a] Chemical shifts ϕ (ppm) are relative to internal $CFCl_3$; since resolution of the spectra was not very high, only the large geminal F–H couplings were observed. [b] Chemical shift values measured from spectra. [c] Data from LTG products; chemical shifts are measured from spectra. See ref 14 and 37.

and TC detection. The photochemical reaction stage consisted of 10 m of 0.015-in. wall, $^3/_8$-in. ID FEP Teflon tubing, one layer wrapped around a 50 mm × 390 mm quartz immersion well containing a 550-W (Hanovia) medium-pressure mercury arc lamp and a second layer wrapped concentrically about an overlying 75-mm Pyrex tube. All FEP Teflon tubing is maintained at approximately 20–25 °C by positive water circulation over all surfaces.

Neopentane Reactions. Reactions F/N-1 through F/N-7 were run on a two-stage modification of the aerosol reactor. This reactor consisted of the reactor with stage-two insert, one staging module without insert followed by the end piece, H, and connecting tubing ($^3/_8$-in. copper tubing). The active volume of this reactor was 321 cm^3 with average diameter of less than 0.5 in. Reaction times were approximated by dividing the active volume of the reactor by the combined flows of gas, principally helium.

Reactions F/N-8 through F/N-12 were run on a four stage modification of the aerosol reactor. This reactor consisted of the reactor with stage-two insert, two staging modules each fitted with staging inserts followed by the end piece, and connecting tubing. The active volume of this reactor was 268 cm^3. The reduced volume is a result of the volume displacement of the second staging insert absent in the first staging module in the previous configuration.

Reactions F/N-13 through F/N-21 were run on the four-stage modification extended by the addition of a 10 m × $^3/_8$ in. copper coil which increased the active volume of this reactor to 771 cm^3. A 15-m coil of $^3/_8$-in. copper tubing and (or) the photochemical module pictured in Figure 1 were the final extensions increasing the active volumes to 1524 and 2108 cm^3 (or 1355 cm^3), respectively. Their effect on reaction times are proportional to the volume changes; however, their effects on product distributions are not nearly so marked as that produced by the first coil. Detailed reaction conditions for each reactor modification are compiled elsewhere.[30c]

In multistaging experiments a gradient in fluorine concentrations was used. For the reactions illustrated in Figures 2–5 an approximate fluorine concentration profile is given in the diagrams of the product distributions. These concentration profiles were calculated by dividing the fluorine flow by the total flow at the end of each reactor stage. Thus they represent the concentrations one would find at these points if no reaction was to occur. The true steady-state fluorine concentration is certainly lower than this value as a result of reaction; the discrepancy will be larger for reactions with high hydrocarbon/fluorine ratios.

The reaction time indicated in these diagrams (Figures 2–5) is the average time required by a suspended hydrocarbon particle travelling from the aerosol generator to the product collecting trap where the fluorination is quenched at −196 °C. This time was calculated from the volume of the reactor and the sum of flows through it. Of course this is only correct if the hydrocarbon remains suspended while it is inside the reactor.

Product mixtures from all neopentane fluorinations were treated with NaF/molecular sieves to remove residual HF. For a check on the performance of every reaction, an analytical GLC injection of a solution of the product mixture in CCl_4 was separated on a $^3/_8$ in. × 7 m 13% fluorosilicone QF-1 (Analabs) on 60–80 mesh chromosorb p column. The following temperature program was used.: T_1 = 25 °C for 10 min, R_1 = 10°/min; T_2 = 75 °C for 10 min, R_2 = 50°/min; T_3 = 125 °C for 24 min.

For identification of the unknown partially fluorinated neopentanes, identical samples from different reactions (as certified byIR) were combined to obtain sufficient material for NMR measurements (Tables I and II), mass spectra, and elemental analysis (supplementary material, Table A). Compounds are ordered NA, NB, ..., NT on the basis of their fluorosilicone QF-1 column retention times (Table III).

Only one fraction from the fluorosilicone QF-1 GLC-separations was further separated. The peak between 33- and 35-min retention time (NO, NP) was separated on a $^3/_8$ in. × 4 m 10% SE-52 phenyl–methylsilicone rubber (Analabs) on 60–80 mesh chromosorb p column by using the following temperature program: T_1 = 70 °C for 10 min, R_1 = 25°/min; T_2 = T_3 = 120 °C for 7 min. Compounds NS and NT occurred in some reactions as a difficult to separate mixture but could be produced nearly pure by stoichiometric control. All purified products prepared for elemental analysis were assayed on the SE-52 column to establish purity after initial QF-1 column GLC purification.

The product distributions for some typical reactions were estimated by determining the areas of peaks in the GLC traces; these data are compiled in Table IV. Since no decomposition during workup was observed and all materials were volatile and soluble in CCl_4, these normalized values should represent something close to the true relative product distributions for the neopentane fluorinations under different reaction conditions. Combining isomers these distributions displayed graphically (Figure 2) show the effect of reaction parameters on fluorination efficiency.

Photochemical Neopentane Reactions. Procedures for conducting the photochemical neopentane reactions (Figure 3) were very similar to the "dark" reactions. As previously was the case, the particulate furnace, cooling jackets, carrier flows, fluorine flows, and, where used, the photochemical cell were allowed to come to equilibrium readiness before any hydrocarbon was admitted to the system. The details of typical photochemical experimental conditions for neopentane, 1,4-dioxane, 2,2-dimethyl-1,3-dioxolane, and cyclohexane are given in Table V, others are detailed elsewhere.[30c] A set of control runs (NPF/N-3 through NPF/N-7) were run under identical conditions except that the photochemical lamp was off. The product distributions of two control runs (NPF/N-3 and NPF/N-6) are illustrated in Figure 3 along with the photochemical runs.

The problems of mass balance in the aerosol system are complex. Through-puts are determined empirically by collecting the output of the hydrocarbon evaporator over several half-an-hour periods. A calibration curve is developed as a function of carrier flow vs. mass output for a given reservoir temperature. Except for those reactions giving only a few products, yields are tedius, time consuming, and prone to experimentalist technique losses. Product distributions as given can be deceiving in that they are yields relative to other products. Generally output masses are about two-thirds of those expected even when no fluorine is used. This points out one of the difficulties of aerosol particulates, i.e., their capture.

Table II. ^1H NMR Spectra of Fluorinated Neopentanes[a]

formula	ref no.	structure	CH_3		CH_2F		CHF_2		integratn ratios
			δ	J,[b] Hz	δ	J,[b] Hz	δ	J,[b] Hz	
C_5H_{12}[c]	*	$C(CH_3)_4$	0.94						
$C_5H_{11}F$	ND	$(CH_3)_3C-CFH_2$	0.96 (d)	1.7	4.0 (d)	48			
$C_5H_{10}F_2$	NL	$(CH_3)_2C(CFH_2)_2$	0.96 (t)	1.8	4.2 (d)	47.6			t:d = 3:2
$C_5H_{10}F_2$	NF'	$(CH_3)_3C-CF_2H$	0.99 (d)	1			~7[c]		
$C_5H_9F_3$	NQ	$(CFH_2)_3C-CH_3$	1.05 (q)	1.7	4.4 (d)	47.1			g:d = 1:2
$C_5H_9F_3$	NK'	$(CH_3)_2C(CFH_2)(CF_2H)$	1.06 (m)	<1	4.25 (d)	47.1	5.67 (t)	56.6	m:d:ı ≈ 7:2:1
$C_5H_8F_4$	NS	$C(CH_2F)_4$			4.6 (d)	46.6			
$C_5H_8F_4$	NN	$(CH_3)_2C(CF_2H)_2$	1.3				~6 (t)		s:t ≈ 3:1
$C_5H_8F_4$	NO	$(CFH_2)_2C(CF_2H)(CH_3)$	1.1		m[e]		5.8 (t)	55.7	s:m:t ≈ 3:4:1
$C_5H_7F_5$	NT	$(CFH_2)_3C-CF_2H$			4.66 (d)	46.6	6.0 (t)	54.7	d:t ≈ 6:1
$C_5H_6F_6$	NR	$(CFH_2)_2C(CF_2H)_2$			4.7 (d)	46.4	6.1 (t)	54.4	d:t = 2:1
$C_5H_5F_7$	NP	$(CF_2H)_3C-CFH_2$			4.9 (d)	46.1	6.2 (t)	54.2	
$C_5H_4F_8$	NK	$C(CF_2H)_4$					6.3 (t)	54	
$C_5H_4F_8$	NI	$(CF_2H)_2C(CF_3)(CFH_2)$			4.95 (d)	46	6.24 (t)	54	
$C_5H_3F_9$	NH	$(CF_2H)_3C-CF_3$					6.3 (t)	53	
$C_5H_3F_9$	NG	$(CF_3)_2C(CFH_2)(CF_2H)$			4.92 (d)	45.6	6.31 (t)	52.2	*f*
$C_5H_2F_{10}$	NE	$(CF_3)_2C(CF_2H)_2$					6.21 (t)	52.2	*f*
$C_5H_1F_{11}$	NC	$(CF_3)_3C-CF_2H$					6.255 (t)	54.5	*f*
C_5F_{12}	NB	$C(CF_3)_4$							

[a] Chemical shifts δ are relative to Me_4Si; they were calculated by assuming that the residual proton on $CDCl_3$ occurs at 7.26 on δ scale. [b] d = doublet, t = triplet, q = quadruplet, m = multiplet (note only basic splittings are given). [c] This signal is a very weak triplet, which does not appear in the print out. [d] From: F. A. Bovey, "Nuclear Magnetic Resonance Spectroscopy", Academic Press, New York and London, 1969. [e] Complex multiplet between 4.3 and 4.6 ppm. [f] Data from LTG products, see ref 14 and 37.

Table III. Identities of Products from Neopentane Fluorinations

ref no.	structure	name
NA	$F-C(CF_3)_3$	perfluoroisobutane
NB	$C(CF_3)_4$	perfluoroneopentane[14,32]
NC	$CF_2H-C(CF_3)_3$	undecafluoroneopentane[32] ≡1-hydryl-*F*-neopentane
ND	$CFH_2-C(CH_3)_3$	1-fluoroneopentane
NE	$(CF_2H)_2C(CF_3)_2$	sym decafluoroneopentane[32] ≡1,3-dihydryl-*F*-neopentane
NF'	$CF_2H-C(CH_3)_3$	1,1-difluoroneopentane
NG	$CFH_2-C(CF_2H)(CF_3)_2$	asym nonafluoroneopentane ≡1,1,3-trihydryl-*F*-neopentane
NH	$CF_3C(CF_2H)_3$	sym nonafluoroneopentane ≡1,1,1,3,3-pentafluoro-2,2-bis-(difluoromethyl)propane
NI	$CF_3-C(CFH_2)(CF_2H)_2$	asym octafluoroneopentane ≡1,1,1,3-tetrafluoro-2,2-bis (difluoromethyl)propane
NK	$C(CF_2H)_4$	sym octafluoroneopentane ≡1,1,3,3-tetrafluoro-2,2-bis-(difluoromethyl)propane
NK'	$CF_2H-C(CFH_2)(CH_3)_2$	asym or 1,1,3-trifluoroneopentane
NL	$(CH_3)_2C(CFH_2)_2$	sym or 1,3-difluoroneopentane
NN	$(CF_2H)_2C(CH_3)_2$	1,1,3,3-tetrafluoroneopentane
NO	$CF_2H-C(CH_3)(CFH_2)_2$	asym tetrafluoroneopentane ≡1,1-difluoro-2,2-bis(fluoromethyl)-propane
NP	$(CF_2H)_3C-CFH_2$	heptafluoroneopentane ≡1,1,3-trifluoro2,2-bis(difluoromethyl)propane
NQ	$(CFH_2)_3C-CH_3$	sym. trifluoroneopentane ≡1-fluoro-2,2-bis(fluoromethyl)-propane
NR	$(CFH_2)_2C(CF_2H)_2$	hexafluoroneopentane ≡1,1,3,3-tetrafluoro-2,2-bis-(fluoromethyl)propane
NS	$C(CFH_2)_4$	sym tetrafluoroneopentane ≡1,3-difluoro-2,2-bis(fluoromethyl)-propane
NT	$CF_2H-C(CFH_2)_3$	pentafluoroneopentane ≡1,1,3-trifluoro-2,2-bis(fluoromethyl)propane
*	$C(CH_3)_4$	unreacted neopentane (2,2-dimethylpropane)

Table IV. Product Distributions from Selected Aerosol Fluorinations of Neopentane (Estimated from Peak Areas of GLC Traces)

	F/N-1	F/N-6	F/N-7	F/N-11	F/N-16	F/N-17	F/N-20	F/N-21
*[a]	4.0	0.5	0.3					
NA						0.3	4.0	4.0
NB						0.6	9.2	9.0
NC						4.4	24.0	19.4
ND	21.8	7.6	3.2					
NE					0.7	11.2	32.6	18.6
NF'	4.3	2.5	1.6					
NG					4.1	5.1	3.3	5.0
NH					3.9	18.9	20.8	14.7
NI					15.7	17.4		10.3
NK'	10.7	10.1	8.7					
NK					12.4	18.7	6.2	10.2
NL	37.9	20.1	10.3					
NM				4.6	9.6	3.5		1.5
NN				1.6	1.5			
NO	6.5	17.4	23.9	14.7	7.4			
NF		2.8	3.8	14.3	6.4			
NP		0.9	1.3	6.1	18.1	15.2		6.5
NO	12.8	16.2	14.0	2.2				
NR		4.1	7.6	24.7	14.9	3.5		0.7
NS	1.8	(3.6)	(5.1)					
		17.8	25.3					
NT		(14.2)	(20.2)	31.8	5.3	1.3		

[a] Unreacted neopentane.

Yields of the photochemical experiments leading to a few products are given. Reaction PF/N-7 yields 0.54 g of *F*-neopentane for 5 h 1 mmol/h run. Theoretical yield estimate for 5 mmol is 1.44 g, a yield of 38%.

1,4-Dioxane Reactions. Although many reactions involving all levels of fluorination of 1,4-dioxane were performed,[30] the instability of the polyfluoro-1,4-dioxanes, especially the trifluoro species, prevented as detailed an examination of product distributions as was detailed for neopentane. Only those reactions (Table V) producing high degrees of fluorine substitution were amenable to even near quantitative workup. In each case the products collected were condensed into a reservoir containing sodium fluoride pellets and L-4A molecular sieves separated by a 1-in. layer of "light" copper turnings and allowed to stand at room temperature overnight. The products remaining were vacuum line fractionated through −78, −131, and −196 °C traps. The −78 and −131 °C traps were combined and subjected to gas chromatographic separation on the fluorosilicone QF-1 column described earlier at a constant temperature of 125 °C. The −196 °C trap, uually containing only a few milligrams of very volatile material, was discarded.

Products from the fluorinations of 1,4-dioxane have been characterized by their ^{19}F and ^1H NMR spectra, CI and EI mass spectra, and IR spectra. As is also the case for partially fluorinated cyclohexanes, ^1H NMR spectra of partially fluorinated 1,4-dioxanes are very complex due

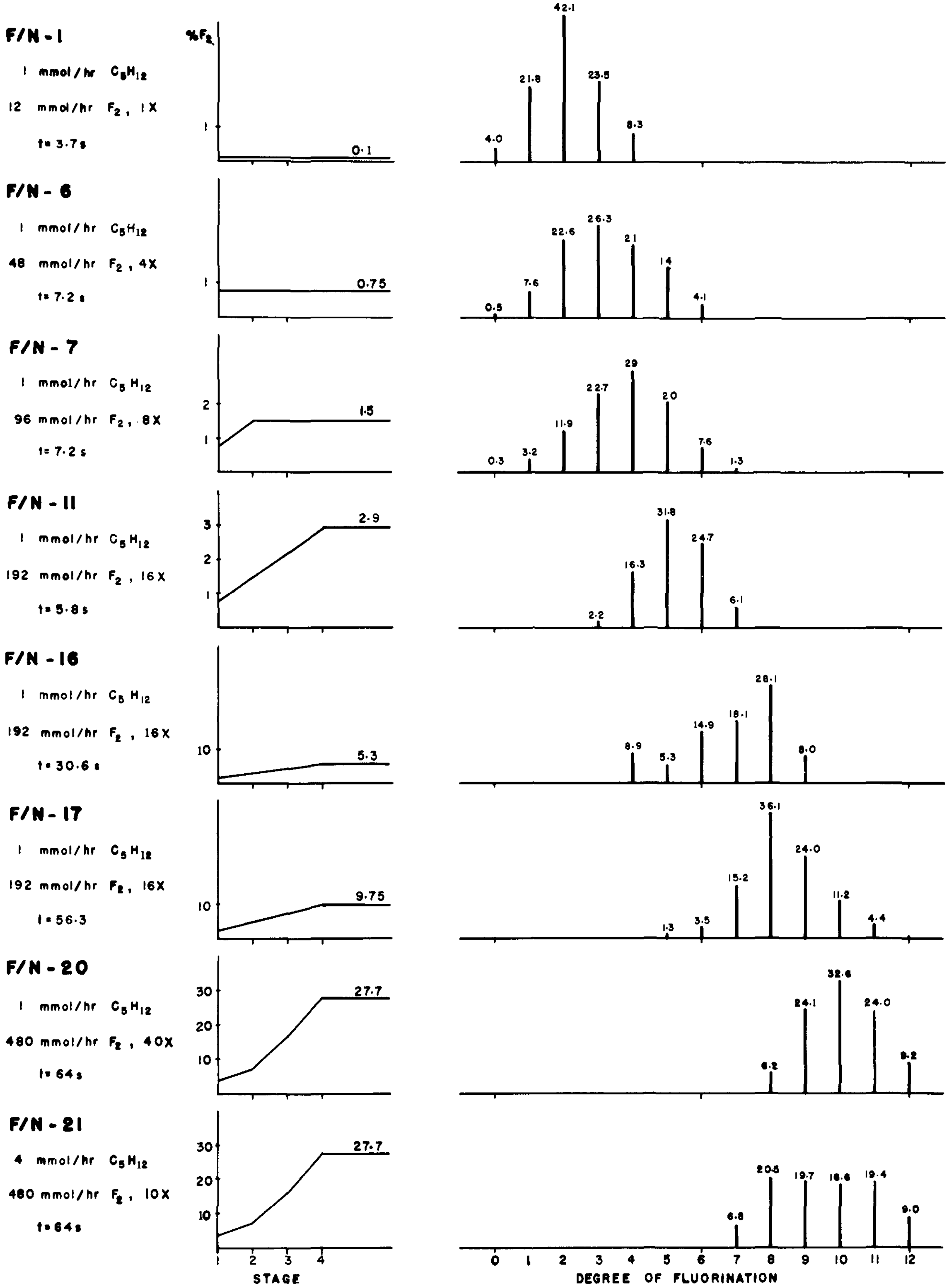

Figure 2. Neopentane product distributions.

to coupling across the ring. But again signals of CH_2 groups and signals of CFH groups can be clearly distinguished, and their relative intgegrations give information about the extent of fluorination.[30a,b] ^{19}F NMR spectra are somewhat less complex. ^{19}F NMR spectra for both the fully and partially fluorinated 1,4-dioxanes containing four or more fluorine atoms have been described in detail in the literature simplifying characterization.[7,32]

---

(32) J. Burdon and I. W. Parsons, *Tetrahedron*, 27, 4553 (1971).

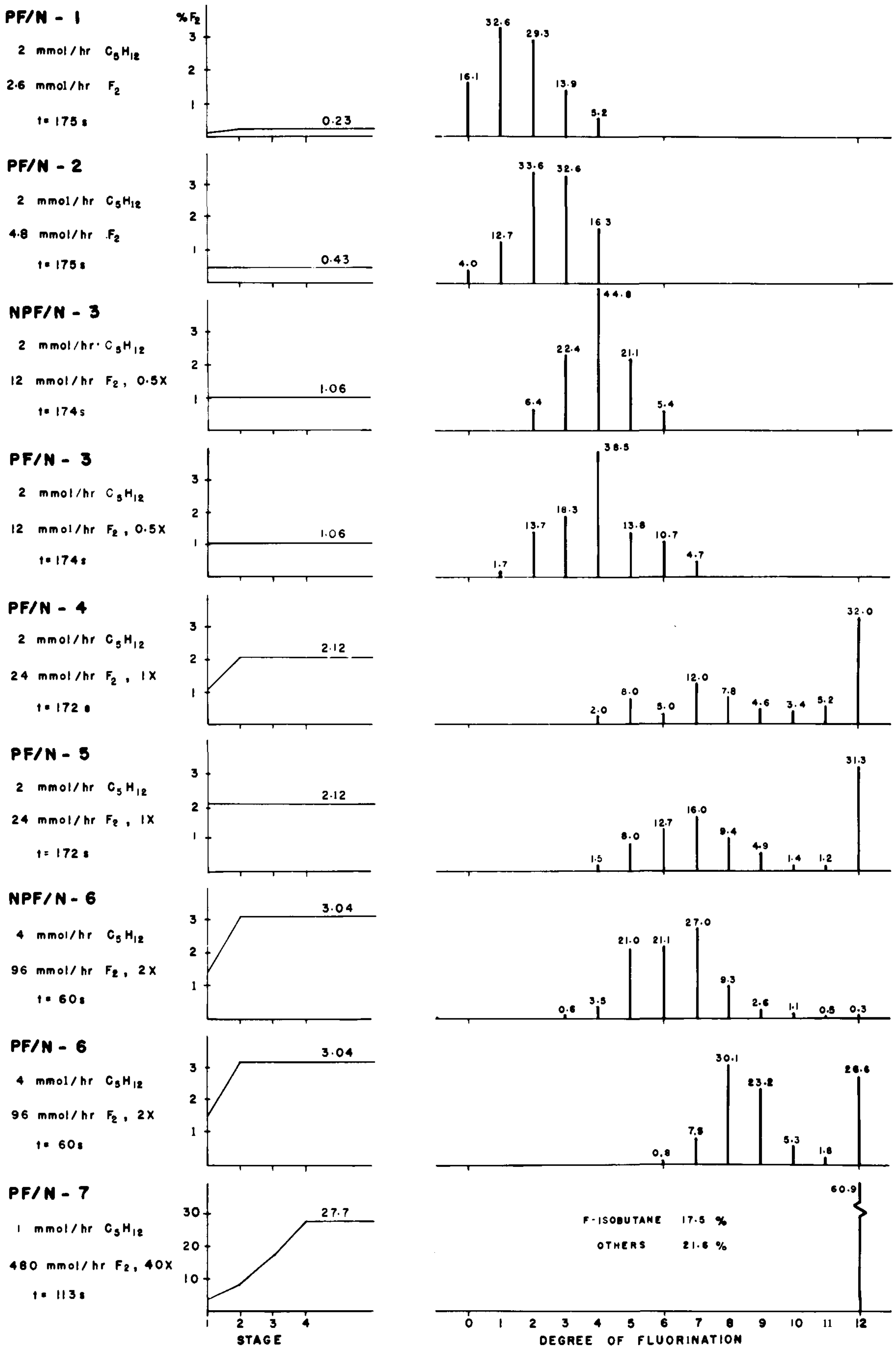

Figure 3. Neopentane photochemical product distributions.

Mass spectra of partially fluorinated 1,4-dioxanes are also very useful for identification; EI mass spectra usually show $C_2F_nH_{4-n}$ masses with very high intensities, from which the number of fluorine atoms on each side of the ring can be determined.[30a,b] This information allowed the product distribution graphs to be readily constructed for reactions producing the more highly fluorinated 1,4-dioxane which may be cleanly separated by single GLC injection (Figure 4). Reaction PF/D-1 produced 0.7963 g of *F*-1,4-dioxane for a 3 h, 2 mmol/h run. Theoretical

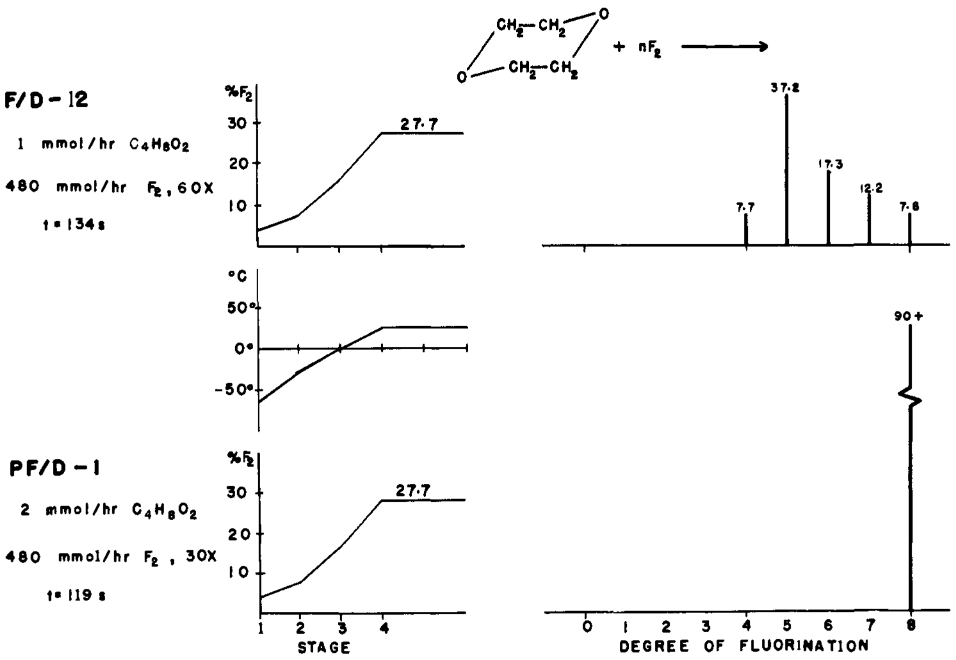

Figure 4. 1,4-Dioxane product distributions.

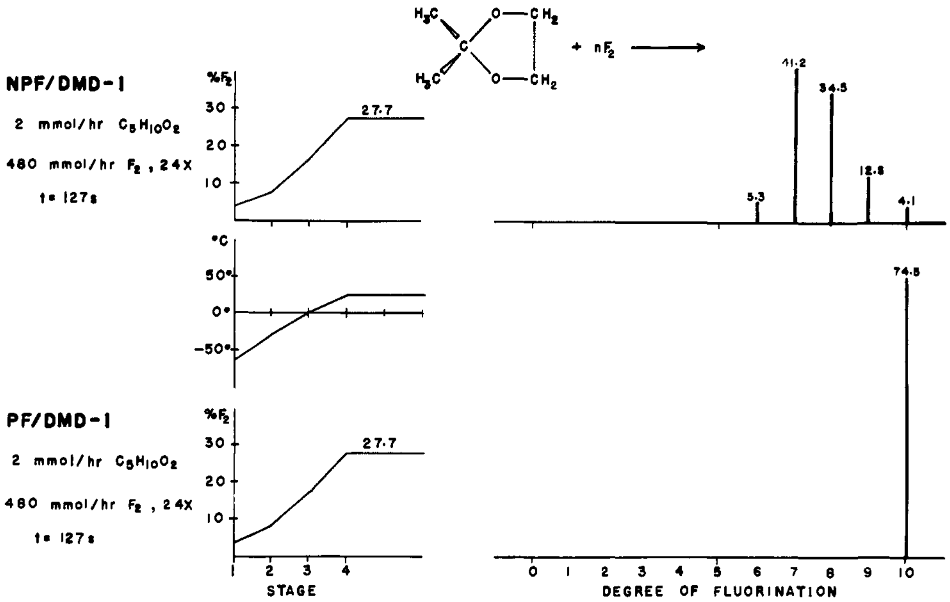

Figure 5. 2,2-Dimethyl-1,3-dioxolane product distributions.

Table V. Reaction Conditions for Photochemical Fluorinations of Neopentane, 2,4-Dioxane (PF/D), Cyclohexane (PF/C), and 2-2-Dimethyl-1,3-Dioxolane (PF/DMD) in the Four-Stage Aerosol Reactor

ref no.	hydrocarbon flow, mmol/h	hc carrier,[a] cm³/min	main carrier, cm³/min	F_2 flows (cm³/min) in stage 1	2	3	4	Σ	F_2 dil He flow, cm³/min
PF/N-7	1	101[a]	400	20	20	60	100	200	4 × 5
PF/D-1	2	63[b]	400	20	20	60	100	200	4 × 5
PF/C-1	2	29[c]	400	20	20	60	100	200	4 × 5
PF/DMD-1	2	20[d]	400	20	20	60	100	200	4 × 5

ref no.	temp (°C) of modules: reactor	no. 1	no.2	coil	hc:F_2	stoichiometry in stage: 1	2	3	4	Σ	% F_2	reactn time, s
PF/N-7	−65	−30	0	RT[b]	1:480	4	4	12	20	40	27.7	113
PF/D-1	−65	−30	0	RT	1:240	3	3	9	15	30	29.3	119
PF/C-1	−65	−30	0	RT	1:240	2	2	6	10	20	30.8	125
PF/DMD-1	−65	−30	0	RT	1:240	2.4	2.4	7.2	12	24	31.2	127

[a] Hydrocarbon reservoir temp: (a) −78 °C, (b) 10 °C, (c) 0 °C, (d) 39 °C. [b] Room temperature.

yield estimate for 6 mmol of *F*-1,4-dioxane is 1.33 g, a yield of 57%.

Cyclohexane Reactions. Again many reactions at virtually all levels of fluorination were conducted with cyclohexane.[30b] The highly complex ^1H and ^{19}F NMR spectra due to extensive coupling and conformational equilibria have been to a great extent worked out in the literature.[33-35] The difficulty in providing meaningful product distributions arises from the difficulties in obtaining quantitative separation of the various products which required use of up to three, generally two, different GLC columns on each complex fraction. For this reason only the photochemical results for conditions (Table V, PF/C-1) leading to perfluorination are reported in this work. The product collected was almost pure *F*-cyclohexane in 30% yield on the basis of average throughput of 2 mm/h.

2,2-Dimethyl-1,3-dioxolane Reactions. Only reaction conditions leading to a high degree of fluorination are tabulated (PF/DMD-1, Table V). Characterization of various hydryl-*F*-2,2,2-dimethyl-1,3-dioxolanes, are given in the literature.[36] The product distributions (Figure 5) represent only those seven major components (~70% total) which are "stable" to the NaF/L-4A treatment and do not pass a -131 °C trap at 10^{-3} torr. The product distributions (Figure 5) are estimates on the basis of gas chromatographic assay on fluorosilicone QF-1 using the temperature separation program $T_1 = -8$ °C for 8 min, heating 8 °C/min, and $T_2 = 144$ °C for 20 min. The photochemical fluorination resulted in collection of 1.1593 g of material at an average hydrocarbon throughput of 2 mmol/h for 3 h. GLC purification of the product gave 0.87 g (74.5%) of pure *F*-2,2-dimethyl-1,3-dioxolane, resulting in a yield estimate of 51.4%.

Results and Discussion

Neopentane, 1,4-dioxane, cyclohexane, and 2,2-dimethyl-1,3-dioxolane have all been successfully fluorinated by the aerosol process. Neopentane, however, was chosen as the model compound for detailed study of the reactor system for several reasons. The most important reasons are the following: all partially fluorinated neopentanes are stable, have a high volatility, and are soluble in CCl_4. There are fewer isomers and only one molecular conformation for each isomer. Gas chromatographic separation in one step has proved to be possible, so that the GLC-chromatogram could be used for quantitative estimation of product distributions. Therefore the influence of reaction parameters should be more easily seen directly from the product distribution. Also four of the most highly fluorinated neopentanes (i.e., *F*-neopentane, undecafluoroneopentane, decafluoroneopentanes, and nonafluoroneopentanes) are known from LTG fluorinations, thus making it easier to judge the "success" of a fluorination.[14,37]

Initially 21 nonphotochemcial reactions with neopentane were run and the results compared.[30] In each of these reactions variables such as carrier flow, fluorine concentration gradient, reaction time, and hydrocarbon mass throughput were changed. Repetitive runs were made, generally only one variable at a time was changed so as to ascertain its effect on product distributions. Examination of all data indicates that the most important variables affecting product distributions are fluorine concentration and reaction time. A comparison of F/N-7 (Figure 2) with NPF/N-3 (no UV control of PF/N-3, Figure 3) establishes this fact. A similar concentration of F_2, a 16:1 excess of fluorine, a 1:24 difference in reaction time give rise to a similar product distribution. A much more efficient use of fluorine. Multistaging accomplishes the expected goal of replenishing fluorine consumed and increasing fluorine concentrations gradually to compensate for increased inactivation of hydrocarbon due to increased fluorine substitution. Multistaging, addition of coils, and decrease of carrier flow all serve to increase reaction time. In none of these reactions was the reactor or reaction uncontrolled or perceptively violent even in those runs involving fluorine flows exceeding 200 cm^3/min (480 mmol/h). The product distributions for typical neopentane fluorinations are given in Figure 2. In this diagram isomers are combined to illustrate the degree of fluorination obtained as a function of fluorine concentration, concentration gradients (i.e., multistaging), relative F_2: hydrocarbon stoichiometry, and reaction time. It is quite evident that a Gaussian distribution of products is approached. This is seen most clearly in reactions F/N-1, F/N-11, F/N-17, and F/N-20. Significant deviations however occur for certain sets of conditions. The most readily explicable is that illustrated by F/N-21, Figure 2. In this reaction only the hydrocarbon throughput was increased (fourfold) relative to F/N-20. This effect, a compression of the maximum toward lower substitution, is probably due to fluorine concentration gradient changes as the increased hydrocarbon throughput consumes additional fluorine; however, mean aerosol particulate size effects could be partly responsible for the spread of products.

Preferential Fluorine Reactivity

The preceding discussion suggests that fluorination occurs stepwise under our conditions and that product distributions with regard to degree of fluorination should be readily explainable on simple statistical and kinetic grounds. The question which remains is whether each degree of fluorination exhibits a distribution of isomers on the basis of simple statistics. In this regard it became necessary to identify each possible isomer, its statistical weight on the basis of the assumption of stepwise fluorination, and the comparison of the theoretical with the experimental distribution of isomers (Table V). Because of the nature of the aerosol process, the assumption that only effects due to statistical weighting or internal directive effects should be important is a defendable one. The basic process involves finely dispersed hydrocarbon particulates in a gaseous helium matrix which are subjected to diffusion controlled attack by gaseous fluorine. Fluorine is injected evenly along the reactor length so as to produce a dynamic fluorine concentration gradient which is ideally at a steady state. Thus the fluorine concentration should remain constant at any given point along the reactor length. This unique set of conditions roughly approximates the conditions produced by a molecular beam apparatus where two reactants intersect and react in a manner governed by condition dependent statistical probability as operated on by the intrinsic reactivities of the reactants themselves. In the aerosol system the intersecting points are random, diffusion controlled, and compound permitting only a statistical treatment and an approximate one at that. It should however be possible to achieve a qualitatively valid comparison between experiment and theory.

The statistical probability of isomers on the basis of the assumption of stepwise substitution are illustrated for neopentane (Figure 6). In each case the probability of the most symmetrical isomer is underlined. The experimentally determined isomer distribution (which is the average of three to five reactions) was determined by comparison of relative peak areas of the gas chromatographed products. In all cases the most unequivocal results are those where two or more isomers are isolated. However single isomer products may be considered at least fivefold probably tenfold larger than any nondetected, nonisolated isomers.

The results indicate that substitution is near statistical until one reaches the pentafluoroneopentane. At this point only the most symmetrical isomer is isolated. This would indicate that a hydrogen of a CH_3 group is more reactive than a hydrogen of a CH_2F or CHF_2 group. At the next step only one hexafluoroneopentane is isolated, indicating that a hydrogen on a CH_2F is more readily substituted than a CHF_2; however this is also statistically the predicted major isomer. The more definitive case comes at the heptafluoroneopentane where again the only isomer isolated is the most symmetrical. However here the unsymmetrical isomer $(CF_3)C(CH_2F)_2(CHF_2)$ is of equal probability. This is a more convincing case for the greater reactivity of hydrogens on CH_2F relative to CHF_2. The octafluoroneopentane case also supports this contention. The theoretical distribution of the unsymmetrical isomer $(CF_3)C(CHF_2)_2(CH_2F)$ to the symmetrical $C(CHF_2)_4$ is 4:1; however the experimental distribution is closer to 1:1. Again at the nonafluoroneopentane the lowered reactivity of the CHF_2 group is indicated in that the ratio of isomers

---

(33) J. Homer and L. F. Thomas, *Trans. Faraday Soc.*, **59**, 2431 (1963).

(34) F. A. Bovey, E. W. Anderson, F. P. Hood, and R. L. Kornegay, *J. Chem. Phys.*, **40**, 3099 (1964).

(35) Jean Cantacuzene and Real Jantzen, *Tetrahedron Lett.*, **37**, 3281 (1970).

(36) R. D. Bagnall, W. Bell, and K. Pearson, *J. Fluorine Chem.*, **9**, 359 (1977).

(37) J. L. Adcock and E. B. Renk *J. Org. Chem.*, **44**, 3431 (1979).

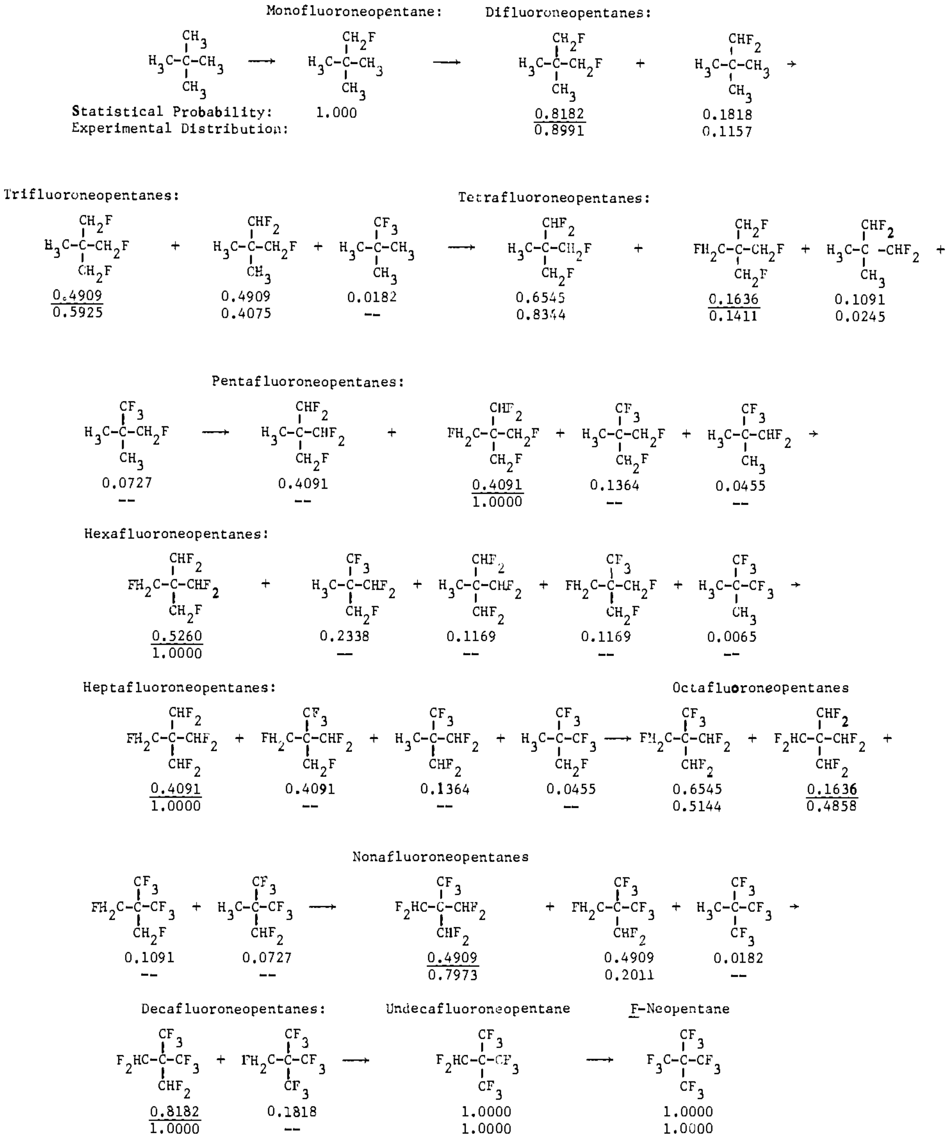

Figure 6. The Statistical probability of Isomers based on stepwise substitution of hydrogens by fluorine.

$(CF_3)_2C(CHF_2)(CH_2F)$ to $(CF_3)C(CHF_2)_3$ theoretically is 1:1; however the experimental ratio is close to 1:4 with the symmetrical isomer predominating.

Although the experimental numbers themselves are of little theoretical value, the experimental isomer ratios compared to the theoretical isomer ratios indicate unequivocally that the reactivities of hydrogen atoms to attack by elemental fluorine can be altered and that hydrogens are not always indiscriminately attacked by fluorine in a purely statistical way. The apparent order of hydrogen reactivity is $CH_3 > CH_2F > CHF_2 \gg CF_3$. This order not only parallels the order of steric accessibility of the hydrogen atoms but also parallels the expected order of electron density on the hydrogens. The latter effect if controlling would indicate that fluorine prefers the more electron-rich hydrogens. This at least suggests that selectivity in a molecule might be achieved by altering the electron density of the carbon bearing the hydrogen.

Photochemical Assisted Fluorinations

The addition of the photochemical reaction stage to the aerosol fluorinator allows the achievement of high degrees of perfluorination although at the expense of some fragmentation (PF/N-7, Figure 3). Yields are still quite high for those "expected" for an elemental fluorine reaction and certainly one utilizing photochemical activation in the final stages. The key to molecular integrity is obviously the fact that molecules entering the gradient photochemical cell are already highly fluorinated (cf. F/N-20 with PF/N-7, Figures 2 and 3) and are therefore more robust and capable of resisting fragmentation under vigorous attack by both molecular and atomic fluorine. It is significant to note that the photochemical cell has not in nearly 1 year of use become befouled and to the contrary looks almost as good as the day it was initiated. A ultraviolet transmission spectrum of the 0.015-in. FEP Teflon film shows that its absorbance curve is near zero and flat until it shuts off at 224 nm in the ultraviolet. It is however of utmost importance to keep the polymer wall near 25 °C as it begins to loose its structural rigidity about 50 °C, forming kinks in the smooth coil. A word of caution is in order; since atomic fluorine is produced in the photochemical cell, excessive temperatures may cause the FEP Teflon to be attacked with disasterous results at the higher fluorine flows.

The higher fluorine flows produce "anomalous" results in the product distributions of the neopentane photochemical reactions. Unlike the "dark" reactions and PF/N-1 through PF/N-3 which give a successively higher degree of fluorination with increasing concentration, PF/N-4 begins to produce *F*-neopentane. The almost identical product distributions in NPF/N-3 (no UV control) and PF/N-3 indicate that in PF/N-1 through PF/N-3 virtually all of the fluorine is consumed by the dark reaction prior to exposure to the ultraviolet irradiation. This finding indicates that hydrocarbons are very reactive to elemental fluorine in the dark at low temperatures but that increasing fluorine substitution deactivates the molecules toward further attack, at least in the kinetic sense. Somewhere between half and complete fluorination molecules become quite resistant to rapid fluorine attack.

A comparison of the control NPF/N-6 with PF/N-6 (Figure 3) indicates that although general upward movement in the product distribution toward higher fluorination occurs, "anomalous" production of *F*-neopentane also occurs. This "anomalous" production of *F*-neopentane in reactions PF/N-4-6 must be due to a "hot molecule" effect. That is, fluorinated neopentanes attacked by atomic fluorine in the photochemical stage become chemically excited and thus more reactive toward fluorine. These "hot molecules" react much more rapidly than nonexcited fluoroneopentanes.

The results seen in reaction PF/N-7 result from two main factors. Molecules are more highly fluorinated when they enter the photochemical stage (cf. F/N-20 (Figure 2) vs. PF/N-7 (Figure 3)), and the fluorine concentration is high enough to exceed the threshold for radical chain propagation throughout the reaction mixture. Both factors contribute toward perfluorination while molecular integrity is maintained to a high degree.

The fluorination of 1,4-dioxane dramatizes the effectiveness of the photochemical stage (Figure 4). The crude product collected from the reactor is better than 90% pure *F*-1,4-dioxane in yields approaching 60%. The extremely difficult direct fluorination of cyclohexane to perfluorocyclohexane can be accomplished in yields exceeding 30% and a product purity in excess of 90% direct from the reactor. The low yields are due to tar formation in stage one which we should be able to eliminate by reducing the fluorine concentration gradient at this stage.

Absence of Hydrogen Fluoride Solvolysis

The direct fluorination reaction produces a molecule of hydrogen fluoride for every hydrogen substituted. It was of interest to determine whether acid-catalyzed cleavage would occur in the reactor system to an appreciable extent. The very acid sensitive ketal, 2,2-dimethyl-1,3-dioxolane, was chosen for this determination. The results indicate that HF solvolysis of such groupings is not a problem. It was possible to produce fluoro analogues of the 1,3-dioxolane in very good yields with almost no evidence of HF solvolysis (Figure 5). The photochemical perfluorination went uneventfully and actually produced higher overall yields than the 1,4-dioxane. Whether this lack of solvolysis is general will, of course, requires reaction of many different compounds possessing different functionalities.

Summary

The multistaged aerosol fluorination reactor achieves near optimum control over the potentially violent direct fluorination reaction. This system meets all of the criteria enumerated earlier which we, by experience, believe contribute to high yield direct fluorination reactions. It additionally has other distinct advantages in that the degree of fluorination may be controlled: it is a flow process, the process is not highly dependent on the physical properties of the reactant to be fluorinated, reactant throughputs may be varied over a considerable range for a given design, fluorine concentration and temperature conditions may be taylored to the reactivity of the reactant, and most importantly the observation of nonstatistical substitution effects suggests that this system might permit the elusive achievement of selectivity in direct fluorinations.

Acknowledgment. This work was supported in part by the Office of Naval Research whose support is gratefully acknowledged. We also wish to thank the Research Corp., Cottrell Research Fund for a starter grant (to J.L.A.), and the South Carolina NMR Facility and Dr. Michelle Buchanan (ORNL) for ^{19}F NMR.

Supplementary Material Available: Table A, IR, mass spectra, and elemental analyses for partially fluorinated neopentanes (7 pages). Ordering information is given on any current masthead page.

Crystal and Molecular Structure of [Tris(4,5-diisopropylimidazol-2-yl)phosphine]dichlorozinc(II)-Bis[*N*,*N*-dimethylformamide]

Randy J. Read and Michael N. G. James*

Contribution from the MRC Group in Protein Structure and Function, Department of Biochemistry, University of Alberta, Edmonton, Alberta, Canada, T6G 2H7.

Received February 3, 1981. Revised Manuscript Received June 29, 1981

Abstract: The crystal structure of [tris(4,5-diisopropylimidazol-2-yl)phosphine]dichlorozinc(II), which crystallized with two molecules of *N*,*N*-dimethylformamide per molecule, has been determined by X-ray methods and refined to a final agreement factor $R = 0.037$ for the 2361 reflections having $I > 3\sigma(I)$. The compound crystallizes in space group *Pnma* with $a = 10.323$ (5) Å, $b = 18.648$ (9) Å, $c = 22.220$ (15) Å, and $Z = 4$. Zn(II) is tetrahedrally coordinated by the N atoms of the three substituted imidazole rings and one of the chloride ions. The molecule has one mirror plane of symmetry which is coincident with the space group symmetry. The title compound is a structural analogue of that part of the active site of the enzyme carbonic anhydrase which consists of Zn(II), three histidine ligands, and a water molecule.

Carbonic anhydrase is a zinc-containing enzyme which catalyzes the reaction

$$CO_2 + H_2O \rightleftharpoons H^+ + HCO_3^-$$

The crystal structures of the isoenzymes from human erythrocytes, human carbonic anhydrases B (HCAB)[1] and C (HCAC)[2], have been determined to 2.2- and 2.0-Å resolution, respectively. These structures show that, in the active site, three histidine residues are coordinated through imidazole N atoms to Zn(II) in an approximately tetrahedral configuration. The fourth ligand is probably a water molecule or hydroxyl ion. [Tris(4,5-diiso-

---

(1) Kannan, K. K.; Nolstrand, B.; Fridborg, K.; Lövgren, S.; Ohlsson, A.; Petef, M. *Proc. Natl. Acad. Sci. U.S.A.* **1975**, *72*, 51-55.

(2) Liljas, A.; Kannan, K. K.; Bergstēn, P.-C.; Waara, I.; Fridborg, K.; Strandberg, B.; Carlbom, U., Järup, L.; Lövgren, S.; Petef, M. *Nature (London), New Biol.* **1972**, *235*, 1-7.

0002-7863/81/1503-6947$01.25/0 © 1981 American Chemical Society